

Effects of Rough Surface on Contact Depth for Instrumented Microindentation Using Spherical Indenter

Ju-Young Kim¹, Jung-Jun Lee¹, Yun-Hee Lee², Jae-il Jang^{3,a} and Dongil Kwon¹

¹School of Materials Science and Engineering, Seoul National University, San 56-1, Sillim-dong, Gwanak-gu, Seoul 151-742, Korea

²Division of Metrology for Quality Life, Korea Research Institute of Standards and Science, 1 Doryong-dong, Yuseong-gu, Daejeon 305-340, Korea

³Division of Materials Science and Engineering, Hanyang University, 17 Haengdang-dong, Seongdong-gu, Seoul 133-791, Korea

^aCorresponding author: jjjang@hanyang.ac.kr

Keywords: Contact depth, Instrumented microindentation, Spherical indenter, Surface roughness

Abstract. Surface roughness is main source of error in instrumented microindentation when it is not negligible relative to the indentation depth. The effect of a rough surface on the results of instrumented microindentation testing using spherical indenter was analyzed by applying the contact depth model, which takes surface roughness into account. Improved variations in hardness and Young's modulus were shown for W and Ni when the results were analyzed by this rough-surface model, while these values were underestimated with increasing surface roughness when analyzed by the flat-surface model. The deformation state of asperities underneath spherical indenter was also discussed.

Introduction

Instrumented microindentation is used extensively to evaluate the mechanical properties of materials in use [1-5]. The most fundamental advantage of instrumented microindentation is that it is unnecessary to measure residual indent by imaging, instead the contact depth h_c is determined from the analysis of the indentation load-depth curve. It is essential that the contact depth model be established precisely since analyzed materials/mechanical properties rely heavily on an accurate determination of contact depth. However, the results of instrumented microindentation are made less accurate in the field by intrinsic error factors such as surface roughness and environmental effects. Since fine surface treatment is in general difficult in the field, surface roughness is an important source of error when it is not negligible relative to the indentation depth [6].

Recently, Kim et al. proposed a rough surface model for use in determining contact depth [7]. We applied the rough surface model to instrumented microindentation using a spherical indenter in this study. Mechanical polishing using diamond paste with various sizes was performed for W and Ni for deliberate control of the surface state. The results obtained by instrumented microindentation were used to analyze hardness and Young's modulus via the current flat-surface model and rough-surface model. The values were found to be independent of the original roughness when the contact depths were analyzed by the rough-surface model.

Rough Surface Contact Model

During microindentation, the material surface underneath an indenter is considered to be microscopically flat and insensitive to the original surface roughness [8]. The asperities inside the projected contact area A_c should be deformed fully plastically as their peaks flow down to fill up their valleys. Initial contact is assumed to happen around the peak of an asperity, since the indenter tip

radius is much larger than that of the asperities. The height at which initial contact occurs is taken as the reference height of the material surface for an ideally flat surface. However, this reference height should be the mean height of surface roughness if the rough surface inside the projected contact area has become smooth in the loaded state. Thus, to determine the contact depth precisely, the difference between the representative height of peaks and the mean height of asperities should be revised.

In mathematical terms, surface heights on a rough surface follow a normal distribution. We thus must determine bounds that in some probabilistic sense cover the individual height values. These bounds can be considered as the representative height of peaks and valleys of asperities. Clearly, a bound that covers the middle 95% of the height distributions is given by mean value \pm standard deviation, which is called a tolerance interval, and indeed the coverage of 95% of the measured height is exact [9]. Thus, the height difference between the representative height for peaks and mean height of asperities is assumed to be 1.96 times the standard deviation. The relation between the average surface roughness R_a and standard deviation σ is $\sigma = \sqrt{\pi/2} \times R_a$ for a normal height distribution. The height difference between the representative peak and mean asperities is 1.56 times R_a , so that the equation for contact depth taking surface roughness into account is

$$h_c = h_{\max} - h_d + h_{\text{pile}} - 2.46 \times R_a \quad (1)$$

where h_d is the height for elastic deflection and h_{pile} is the height for pile-up/sink-in. The schematic of the rough surface model is presented in Fig. 1.

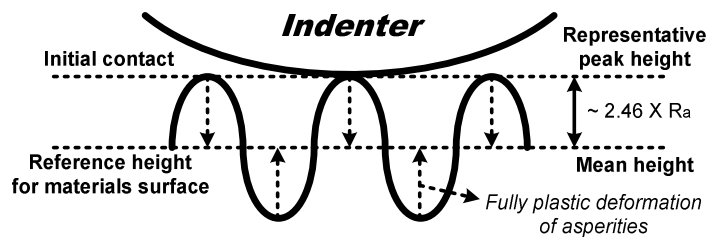


Fig. 1. Schematic of rough-surface model.

Experiments

We prepared 99.99% Ni and 99.9% W samples and polished their surfaces with 9, 6, 3, 1, and 0.25 μm diamond paste. Their surfaces were examined by optical profiler with depth resolution 0.1 nm to measure the degree of surface roughness. Instrumented microindentation tests using a spherical indenter with radius 250 μm were performed on the samples with indentation depth 50 μm , using an AIS 3000 (Frontics Inc.) with load resolution 5.6 gf and depth resolution 0.1 μm . The zero index, considered as initial contact in the equipment, was set as twice the depth resolution for accurate detection of initial contact. The residual indents were then examined by optical profiler to measure the heights of pile-up/sink-in.

Results and Discussion

Morphology of Surface and Residual Indent. R_a values were measured by optical profiler with depth resolution 0.1 nm: the results were $0.050 \pm 0.019 \mu\text{m}$ for 9- μm diamond paste, $0.311 \pm 0.010 \mu\text{m}$ for 6- μm diamond paste, $0.500 \pm 0.044 \mu\text{m}$ for 3- μm diamond paste, $1.154 \pm 0.238 \mu\text{m}$ for 1- μm diamond paste, and $1.712 \pm 0.0573 \mu\text{m}$ for 0.25- μm diamond paste. The residual indents were assessed as h_{pile} of $7.03 \pm 0.51 \mu\text{m}$ for W (pile-up) and $3.67 \pm 0.49 \mu\text{m}$ for Ni (sink-in), as shown in Fig. 2. Pile-up/sink-in occurs only by plastic deformation during indentation, so h_{pile} as obtained from the residual indent could be used in calculating Eq. (1) in the loaded state.

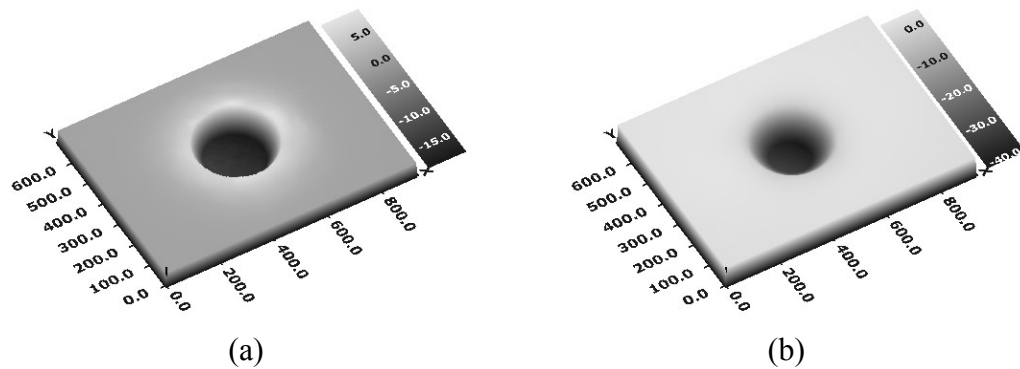


Fig. 2. Residual indents measured by optical profiler for (a) W (pile-up) and (b) Ni (sink-in).

Hardness and Young's Modulus. The variations in hardness and Young's modulus analyzed by the current flat-surface model are shown in Fig. 3. These values were underestimated more and more as the average surface roughness increased, although hardness and Young's modulus should be independent of original surface roughness. When the maximum difference in R_a is $1.66 \mu\text{m}$, the hardness and Young's modulus of W decreased by 4.97% and 3.70%, respectively, and those of Ni decreased by 5.76% and 3.87%, respectively. The open circles in Fig. 3 show the same data as analyzed by the rough-surface model and show negligible variation with average surface roughness compared to the values analyzed by the flat-surface model. The averages and standard deviations of the values analyzed by the rough-surface model were 4.99 ± 0.02 GPa for hardness of W, 309.6 ± 1.3 GPa for Young's modulus of W, 1.57 ± 0.01 GPa for hardness of Ni, and 188.36 ± 0.88 GPa for Young's modulus of Ni. It can be concluded that the rough-surface model yields the hardness and Young's modulus values insensitive to the original surface roughness, while these values were underestimated in the flat-surface model more and more with increasing average surface roughness, since the maximum load and stiffness measured by instrumented microindentation using spherical indenter decreased and the variation in analyzed contact area becomes negligible with increasing average surface roughness [7].

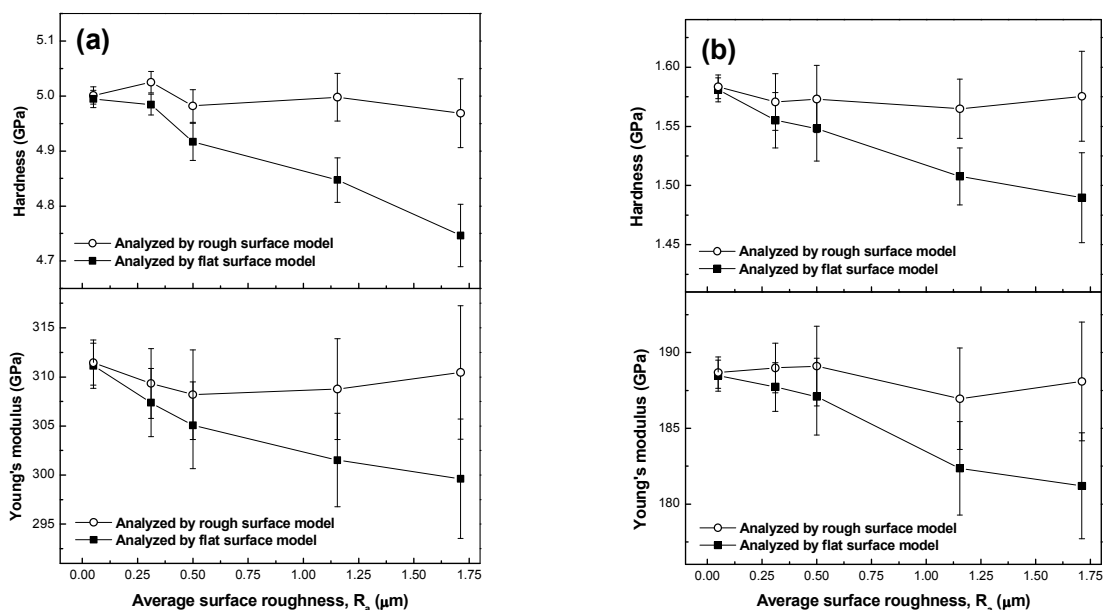


Fig. 3. Hardness and Young's modulus for (a) W and (b) Ni with average surface roughness.

Deformation of Asperities. The asperities contacted beneath an indenter are flattened by fully plastic deformation. Zhao et al. proposed distinguishing among elastic, elastic-plastic, and fully

plastic deformation of asperities indented by a rigid flat indenter [10]. This model can be applied in general indentation experiments since the indenter material is usually much more rigid than the indented materials and the indenter radius is generally greater than that of the asperities. The criterion for fully plastic deformation is given as $486\pi^2 K^2 H^2 R_{asp} / 16E^2$, where K is a dimensionless constant, H and E are the material hardness and Young's modulus, and R_{asp} is the radius of asperities. The value of this criterion was calculated as about 0.03 times of R_{asp} for ductile materials by using the rough values $K = 0.3$, $H = 1$ GPa, and $E = 100$ GPa. From this it was concluded that the asperities are deformed fully plastically from very early contact (relative to the asperity radius).

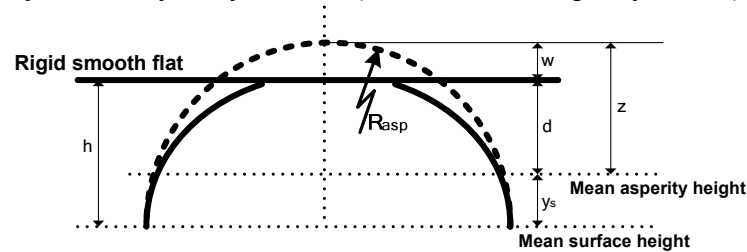


Fig. 4. Deformation state of asperities indented by rigid flat indenter.

Conclusions

The rough-surface model for determining contact depth was used in instrumented microindentation tests with a spherical indenter. Hardness and Young's modulus analyzed by the current flat-surface model were underestimated more and more as average surface roughness increased. However, the variation in hardness and Young's modulus analyzed by rough-surface model is both small and insensitive to original surface roughness. The feasibility of the rough-surface model for instrumented microindentation tests using a spherical indenter was verified experimentally. It was also confirmed that the asperities indented by a spherical indenter deform fully plastically from very early contact relative to the asperity radius.

Acknowledgments

This research was supported partly by a grant (code #:06K1501-01111) from the *Center for Nanostructured Materials Technology* under the *21st Century Frontier R&D Program* of the Ministry of Science and Technology, Korea, and partly by a grant (code #:10023468) from the *Standardization R&D Program* of the Ministry of Commerce, Industry and Energy, Korea.

References

- [1] J.-Y. Kim, K.-W. Lee, J.-S. Lee and D. Kwon: *Surf. Coat. Technol.* (accepted for publication)
- [2] W.C. Oliver and G.M. Pharr: *J. Mater. Res.* Vol. 7 (1992), p. 1564
- [3] J.-i. Jang, Y. Choi, Y.-H. Lee and D. Kwon: *Mater. Sci. Eng. A* Vol. 395 (2005), p. 295
- [4] Y.-H. Lee and D. Kwon: *Acta Mater.* Vol. 52 (2004), p. 1555
- [5] J. Pullen and J.B.P. Williamson: *Proc. R. Soc. Lond. A* Vol. 327 (1972), p. 159
- [6] J.-Y. Kim, B.-W. Lee, D.T. Read and D. Kwon: *Scripta Mater.* Vol. 52 (2005), p. 353
- [7] J.-Y. Kim, J.-J. Lee, Y.-H. Lee, J.-i. Jang and D. Kwon: *J. Mater. Res.* (submitted for publication)
- [8] K.L. Johnson: *Contact Mechanics* (Cambridge University Press, UK 1985)
- [9] R.E. Walpole and R.H. Myers: *Probability and Statistics for Engineers and Scientists* (Prentice Hall, USA 1993)
- [10] Y. Zhao, D.M. Maietta and L. Chang: *ASME J. Tribol.* Vol. 122 (2000), p. 86